An analysis of limits for part load efficiency improvement with VVA devices

Vincent Knop, Leonardo Mattioli

An analysis of limits for part load efficiency improvement with VVA devices

Vincent Knop *, Leonardo Mattioli

IFP Energies nouvelles, 1 et 4 avenue de Bois-Préau, 92852 Rueil-Malmaison, France

The implementation of Variable Valve Actuation (VVA) in Spark-Ignition (SI) engines generally aims at increasing part-load efficiency by reducing pumping losses. However, any innovative valve strategy has effects on the combustion process itself, introducing new limitations and mitigating the fuel consumption benefits. The experimental analysis of such valve strategies identifies the optimum settings but does not explain the origin of benefits and the sources of unexpected drawbacks. In the present study, the experimentally-optimised operating conditions for different valve strategies were numerically compared with 3D CFD to gain knowledge about causes for efficiency benefits and consequences of valve strategy on combustion progress.

We compared standard SI operation in a single-cylinder port-fuel injection gasoline engine to mixture leaning, early intake valve closure (Miller cycle), late intake valve closure (Atkinson cycle), as well as Controlled Auto-Ignition (CAI). All alternative methods reduced pumping work and improved fuel consumption. However, all alternative methods also altered combustion progress and thermodynamic state within the combustion chamber, so that the observed fuel consumption benefits never reached the expected values. An energy balance provided the additional losses induced by each strategy while in-cylinder turbulence and temperature quantification helped explain the trends in combustion speed.

1. Introduction

Variable Valve Actuation (VVA) is not a new technology as BMW introduced the Valvetronic system in 2001 to obtain a throttle-free load control [1]. Many other car manufacturers since introduced similar systems that mostly rely on the scaling or on the truncation of the valve lift profile and therefore on the early closure of the intake valve(s) [2–5].

Although efficient to reduce pumping losses, the Early Intake Valve Closure (EIVC) reduces turbulence intensity, turbulent kinetic energy being converted into heat when valves are closed as there is no momentum source to compensate for the viscous losses in the trapped air charge [6,7]. The lower the load, the earlier the EIVC for throttle-free load control, so that turbulence dissipation from EIVC to Bottom Dead Center (BDC) increases. The EIVC strategy is therefore less and less efficient with load reduction as the lack of turbulence slows down flame propagation [8]. Efficient idling becomes a challenge as combustion stability is poor [9], while it is an important operating point for both driving cycles and real-life driving.

Cylinder head and piston modifications to create masks can partly compensate for the EIVC-induced turbulence dissipation at part load [10]. However, at full load, masking interferes with the trade-off between flow capacity and tumble motion creation, limiting turbulence level at spark ignition and impeding combustion efficiency as well as power output. With its Valvetronic system, BMW additionally implemented the differentiation of intake valve lift profiles at lower part loads, generating some swirl motion within the combustion chamber to improve combustion stability [11]. Although not as efficient as tumble motion to help mixing and flame progress, swirl motion has the advantage of not being dissipated at the end of compression, so that some motion survives even in the worst conditions. A third measure to sustain idling operation with short valve opening duration is a late intake valve opening, providing a throttle-free control of engine load, while restricting the extent of burnt gas trapping and increasing the turbulence level at spark timing (higher velocities through valves and less time for turbulence dissipation) [5,12]. This latter method produces more pumping losses than the EIVC method but the improvement of combustion quality largely compensates for the additional pumping losses in the energy balance.

The alternative to EIVC for pumping loss reduction is Late Intake Valve Closure (LIVC) that minimises turbulence conversion into

* Corresponding author. Fax: +33 147526685.
E-mail address: vincent.knop@ifpen.fr (V. Knop).

heat but can destroy a part of the structured flow motion during the added backflow to the intake pipe [7]. The restriction in structured flow motion limits its conversion into turbulence during the second part of the compression stroke. Nevertheless, LIVC has the double advantage over EIVC of less turbulence penalty at ignition timing and of less sensitivity to intake port design [7]. LIVC deficiencies are the necessary work done to induct some mass that is immediately pumped back out, and the cycle-to-cycle heating and dilution of intake gases by the backflowed gases [13], which has important implications on heat transfer and combustion. LIVC also implies a lower end-of-compression temperature, which is beneficial to reduce knock propensity at higher loads [14,15] but is detrimental to combustion speed and stability at part load [7,8,16].

When both intake valves are identically operated, LIVC has more potential in the lower load range and moderate turbulence level, due to the lower impact on combustion and hence the maximum dethrottling at the latest possible intake closure timing. As the load increases, less turbulence is required, and so the EIVC method produces the best results, mainly due to reduced friction caused by the smaller valve lift [2,7].

Although those trends are well-known through various studies [10,13–16], there is a lack of published quantification of the effect of IVC timing on a single setup at part load operation, including the influence on combustion and a detailed energy balance. Deficiencies on combustion are known but seldom quantified, so that they cannot be explicitly included in optimisation algorithms such as the work of Atashkari et al. [17]. Consequently, optimisation algorithms can only be used on restricted variable valve timing amplitudes to only refer to conditions where combustion remains stable and without any first order effect on global efficiency. Similarly, some additional secondary losses have been identified but not clearly quantified in a complete energy balance, so that trends for future engine optimisation remain unknown. As a matter of fact, the energy balance shift with the different VVA strategies leads to different engine optimisation strategies for future engine efficiency optimisation.

As more and more complex VVA systems are available in series SI engines, implementation of alternative combustion modes like Controlled Auto-Ignition (CAI) or gasoline Homogeneous Charge Compression Ignition (HCCI) becomes possible at almost no additional cost. Such an implementation, however, requires to gain a good control over the heat release and to establish a clear fuel consumption benefit and/or a clear way to potentially reach further fuel consumption benefits. It was therefore very interesting to include such a combustion mode in the present analysis. In the present study, we concentrated on typical negative valve overlap operation with similar valve lift profiles for both intake valves to maintain a similar level of complexity to that of SI operating strategies. A further step in reduction of pumping losses could be reached in a future study introducing the specific valve strategy of Mahrous et al. [18] that differentiates the intake valve profiles to avoid the direct link between intake and exhaust valve lift timings.

Fuel consumption improvement in gasoline engines can be driven by other methods than mixture leaning or valve actuation alteration [8]. Such alternative methods are either already part of the present engine setup (downsizing) or cannot be implemented in the existing layout (variable compression ratio, stratified charge operation). All that methods can also be combined to reach some synergy [8]. However, present results show that, when pushed to the extreme, selected methods for fuel consumption reduction cannot be added because they all lead to a strong combustion degradation.

In the following, we compared various VVA strategies on a single part-load operating point in terms of fuel economy and of secondary losses that restrict the benefits with respect to early expectations. The alteration of the energy balance when changing the operation strategy was also examined to point out where future work should be directed to enlarge fuel consumption benefits.

2. Experimental setup and engine specifications

The present study relied on a 4-valve pent-roof port-fuel-injection single-cylinder research engine with a displacement of 0.5 l and a geometrical compression ratio of 12.0:1. Table 1 summarises its main geometrical characteristics. The Actuating Valve Train (AVT) system from Lotus engineering [19] independently controls the motion of each valve. This electro-hydraulic system has a large number of parameters to define the valve lift profile: peak valve lift, opening and closure duration, as well as opening and closure timing. Previous studies performed with this engine and its variable valve actuation device provide further details [20–22].

The engine was equipped with an AVL noise-meter (AO1) and crank-resolved pressure transducers in the intake pipe (Kulite XT-123B-190-50A), in the cylinder (AVL QC33D), and in the exhaust pipe (AVL QC43D) to fully monitor the gas exchange process and to define CFD boundary conditions. The pressure transducers were located as close as possible to the cylinder head flange, *i.e.* 200 mm upstream the intake valves on the intake side and 140 mm downstream the exhaust valves on the exhaust side. Raw emissions (uHC, NO_x, CO, CO_2, and O_2) were measured with a standard 5-gas analyzer (AVL AMA i60). Fuel metering combined direct weighting and fuel flow rate computations based on air flow rate measurements with sonic nozzles and Fuel/Air Equivalence Ratio (FAER) quantifications. The FAER quantification relied on an analysis of the exhaust gas composition based on uHC, NO_x, CO, CO_2, and O_2 concentrations. Both methods were checked for consistency at each operating point to detect possible defects.

3. Operating strategies

Table 2 details the 5 selected operating strategies to reach a reference condition within the urban part of the NEDC homologation cycle, namely the 2000 rpm – 3 bar Indicated Mean Effective Pressure (IMEP) operating point. First four strategies were standard spark-ignited combustion with flame propagation and explored benefits related to mixture leaning and VVA. Last strategy was the alternative CAI combustion mode [20–22] relying on air–fuel mixture auto-ignition and kinetically-controlled heat release.

First strategy was the conventional spark-ignition operation with a stoichiometric mixture and an intake valve closure just after Bottom Dead Center (aBDC). This operating point was the reference for comparison with other strategies and outlined the well-known deficiencies of spark-ignited engines: load control with throttling induces large pumping losses that impede the Indicated Specific Fuel Consumption (ISFC). All other strategies aimed at improving the overall efficiency by reducing pumping losses.

Second strategy was mixture leaning, improving efficiency through reduced pumping losses and improved thermodynamic properties. Such a strategy is not related to a VVA device but was

Table 1
Main engine specifications.

Bore (mm)	82.7
Stroke (mm)	93.0
Conrod length (mm)	143.0
Compression ratio (–)	12.0:1

Table 2
Comparison of experimental results for all 5 operating strategies on the 2000 rpm – 3 bar IMEP operating point.

Strategy		Reference	Leaning	Atkinson	Miller	CAI
Engine speed	rpm	2000	2000	2000	2000	2000
IMEP	bar	3.0	3.0	3.0	3.0	3.0
Fuel/Air equivalence ratio	–	1.0	0.8	1.0	1.0	1.0
IVC at 1 mm valve lift	cad aBDC	35	35	110	−60	22
Effective compression ratio	–	11.3	11.3	5.4	9.9	11.7
Avg. intake manifold pressure	bar	0.370	0.422	0.633	0.540	0.932
Air mass flow rate	kg/h	9.5	11.3	8.9	8.9	8.7
PMEP	bar	−0.692	−0.671	−0.462	−0.605	−0.342
Spark timing (CA_{ign})	cad bTDC	23	27	36	29	–
$CA_{10} - CA_{ign}$	cad	21.6	26.3	32.3	27.3	–
$CA_{90} - CA_{10}$	cad	26.2	26.8	35.3	34.4	10.5
Std. dev. on CA_{50}	cad	2.8	4.2	2.8	2.9	1.2
Std. dev. on IMEP	%	1.4	2.3	1.5	2.0	2.6
Std. dev. on peak pressure	%	8.8	14.2	9.1	9.4	2.6
ISFC	g/kW h	262.7	250.3	250.6	250.2	242.9
Indicated efficiency	%	32.0	33.6	33.6	33.6	34.6
Avg. exhaust runner pressure	bar	1.008	1.013	1.008	1.010	1.059
Avg. exhaust runner temperature	°C	570	525	555	575	379
Engine-out uHC emissions	g/kW h	5.8	6.0	5.6	5.1	3.5
Engine-out CO emissions	g/kW h	14.5	4.0	14.2	12.3	21.7
Engine-out NO_x emissions	g/kW h	11.1	8.9	9.2	9.2	0.4

considered as an alternative way to improve fuel economy and as a potential synergistic solution to combine with a VVA approach. Firstly, mixture leaning requires a larger air mass flow rate for a given fuel mass flow rate and therefore a higher intake pressure, which reduces pumping losses on part-load operating points. Secondly, mixture leaning increases the γ-value of the air–fuel mixture, therefore increasing the theoretical thermodynamic efficiency and reducing heat losses to the walls through a restricted mean in-cylinder temperature. For the present analysis, we selected a FAER value of 0.8 based on a FAER sweeping from 0.7 to 1.0 with steps of 0.05. Further leaning at test bench degraded so much combustion speed that fuel consumption raised again. The measured fuel consumption benefit for a fuel/air equivalence ratio of 0.8 was 12 g/kW h and result analysis showed that pumping loss reduction was modest (only 0.02 bar benefit in PMEP). Beyond the fuel consumption benefit, mixture leaning also provided a 70% benefit in engine-out CO emissions and a 20% benefit in engine-out NO_x emissions. Nevertheless, lean exhaust gases imply a poor efficiency for NO_x aftertreatment within the 3-way catalyst, so that the tail-pipe NO_x emissions raise without any specific de-NO_x device implementation.

Third strategy was Aktinson cycle: intake valves closed late in the compression stroke, so that part of aspirated gases flowed back into the intake port. Part-load efficiency is improved because a larger air mass must be aspirated during the standard intake stroke, leading to a higher intake pressure and reduced pumping losses. A sweeping in IVC timing up to 130 cad aBDC with steps of 10 cad provided the fuel-economy-optimised IVC of 110 aBDC. The selected operating point was the latest intake valve closure before combustion degradation reduced indicated efficiency. The same fuel consumption benefit (12 g/kW h) as mixture leaning was measured, while mixture remained stoichiometric and exhaust gas aftertreatment remained efficient. LIVC restricted the effective compression ratio down to 5.4 (see Table 2) and backflow destroyed a part of the structured flow motion. At compression end, mixture was therefore cooler and less turbulent, both impeding combustion speed. A benefit of mixture cooling was the reduction in engine-out NO_x emissions, while maintaining the exhaust gas aftertreatment efficiency. Choosing between mixture leaning and LIVC is therefore a matter of cost-effectiveness between a VVA device and a de-NO_x device, implementation being easier for the de-NO_x device.

Fourth strategy was Miller cycle: intake valve closed early in the intake stroke, requiring a higher intake pressure to aspirate the same air mass within a shorter induction period. A sweeping in IVC timing up to −100 cad aBDC provided the fuel-economy-optimised IVC of −60 cad aBDC. Miller cycle also produced a reduction in pumping losses but to a smaller extent than Atkinson cycle because combustion degradation was too important for earlier intake valve closure. Despite the smaller benefit in pumping losses, a similar fuel consumption benefit (12 g/kW h) as for both previous strategies was measured, which is coherent with previously published results [8]. Combustion duration increase and engine-out NO_x emission decrease were similar to that of Atkinson cycle. Choosing between mixture leaning, EIVC and LIVC is therefore again a matter of cost-effectiveness.

Fifth strategy was CAI combustion mode obtained with burnt gas trapping through negative valve overlap [20–22]. Operation was almost completely unthrottled and pumping losses were largely reduced, but not removed as will be discussed later on. Combustion was also very short (60% shorter than for the reference SI operating point), so that fuel consumption benefit (20 g/kW h) was larger than for any SI operating point. The very large dilution rate provided an additional significant benefit for engine-out NO_x emissions (96% reduction with respect to the reference SI operating point). Engine-out unburnt hydrocarbon emissions were lower by 40% but CO emissions were higher by 50% compared to the reference operating point. Mixture stoichiometry ensured a large reduction in emissions within the 3-way catalyst but the significantly lower exhaust temperature might become an issue for catalyst light-off.

Fig. 1 details the selected valve lift profiles for each strategy. It is noteworthy that Miller and Atkinson cycles were here compared to standard operation without any change in valve overlap, which might lead to differences with some literature results obtained with a variable valve timing device.

The implementation intent for all 5 strategies was a complete pumping loss removal in order to improve the overall efficiency. A removal of pumping losses without any other side effect would decrease fuel consumption by 20%. We did not measured such a

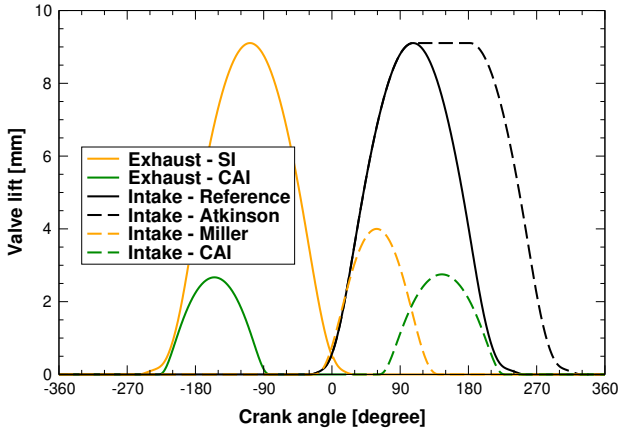

Fig. 1. Valve lift profile for each operating strategy.

large fuel economy because additional losses occured and valve strategy alteration impeded combustion for SI operating points, limiting the dethrottling extent. Such losses were the survival of some pumping losses, combustion degradation and/or modification of heat losses to the walls or to the exhaust. The main objective of present paper was to quantify such additional losses in order to identify the best counter-measures for each operating strategy.

4. Global behaviour

Fig. 2 depicts the pressure trace for each operating strategy and outlines the large difference in engine behaviour between SI cases and CAI case. CAI operation was the only fully unthrottled operating strategy but such a dethrottling level relied on the trapping of a large quantity of burnt gases (truncated exhaust – Fig. 1). The truncated exhaust and the larger trapped mass induced a significant increase in pressure during the compression stroke, but also the occurrence of a second compression event during negative valve overlap (last 90 cad before 720 cad and first 90 cad after 0 cad). The higher pressure (related to the larger trapped mass) and the higher temperature (related to the trapping of hot burnt gases from the preceding engine cycle) promoted fuel reactivity and ensured auto-ignition occurrence.

For SI operating points, behaviour differences were hardly visible in Fig. 2 but were better outlined with a $p - V$ diagram (Fig. 3). Mixture leaning or valve strategy alteration changed the low pressure part of the diagram but some pumping losses remained clearly visible. Mixture leaning notably did not lead to a large gain in pumping losses, so that the fuel economy improvement is exclusively related to the high pressure part of the diagram. Atkinson cycle seemed to generate larger gains than Miller cycle but impeded the earlier compression. Pumping losses computed by integration between consecutive BDC indicated a larger gain for Atkinson cycle than for Miller cycle but the full cycle indicated efficiency was identical for both cycles. For CAI operation, unthrottled operation should remove pumping losses but some subsisted, as previously observed elsewhere [18,23]. In fact, most flow-motion-induced pumping losses were removed but heat-loss-induced pumping losses were created because of the high in-cylinder temperature during the second compression.

An energy balance, issued from the experimental pressure trace, the known piston law, the thermodynamic state of the trapped mixture, and the heat losses computed with the Woschni model [24], provided the instantaneous energy flow that occurred during combustion. Such a combustion analysis of experimental pressure traces indicated a degradation of combustion for any of the alternative SI operating strategies (Table 2). When leaning the mixture, the main combustion event ($CA_{90} - CA_{10}$, 10–90% of burnt mass fraction) remained unaltered but combustion initiation ($CA_{10} - CA_{ign}$, ignition to 10% of burnt mass fraction) was significantly slower. This may, however, be compensated for with an adapted ignition timing. On the contrary, for VVA strategies, optimising fuel consumption benefits required to go as far as possible into combustion degradation before it overcame pumping loss benefits. For such operating points, the complete combustion event worsened as mixture temperature and turbulence decreased, impeding the laminar flame speed and the flame propagation enhancement by turbulence.

5. Numerical analysis

Pressure trace comparison and combustion analysis provided some experimental inputs about the influence of each operating strategy on engine behaviour but there was a lack of quantitative information to explain the reasons for the longer combustion duration with alternative operating strategies. To gain additional knowledge, we performed a 3D CFD analysis of all 5 operating points and analysed the implications of valve strategy change on turbulent velocity, species and temperature fields. Such an analysis indicated the reason for the alteration of combustion speed. Complete engine cycles were computed so that a detailed analysis of CFD results also provided a complete energy balance, giving insights about the unexpected new losses and about their relative influence.

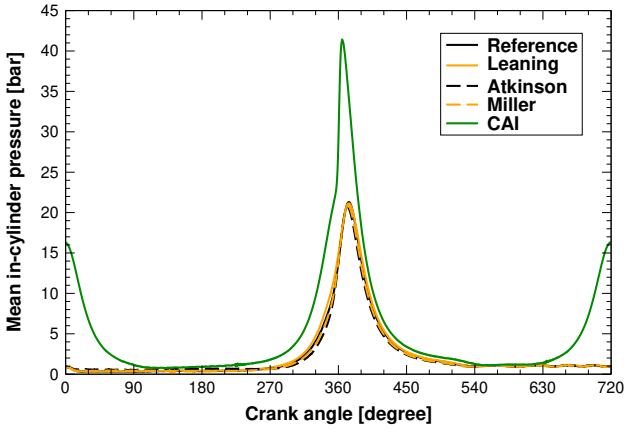

Fig. 2. Mean in-cylinder pressure trace for each operating strategy.

5.1. Engine CFD code

The 3D CFD computations relied on an in-house code called IFP-C3D [25]. This code is a RANS parallel (MPI) solver for reactive compressible gas flows with sprays dedicated to multi-physics three-dimensional simulations of internal combustion engines. When dealing with SI engines, detailed in-house models for spark ignition [26], flame spreading [27,28], auto-ignition detection [29] and pollutant formation including detailed chemical kinetics information [30] are considered. Turbulence modelling relied on the k–ϵ RNG model [31] and the law-of-the-wall on the model of Kays and Crawford [32]. Present computations included meshes with a typical cell size of 0.5 mm and described the complete 4-stroke engine cycle, performing a multicycle computation for operating points with cycle-to-cycle coupling (Atkinson cycle and CAI combustion mode). MPI parallelism within IFP-C3D provides a linear speed-up up to at least 128 processors [33] and therefore short elapsed

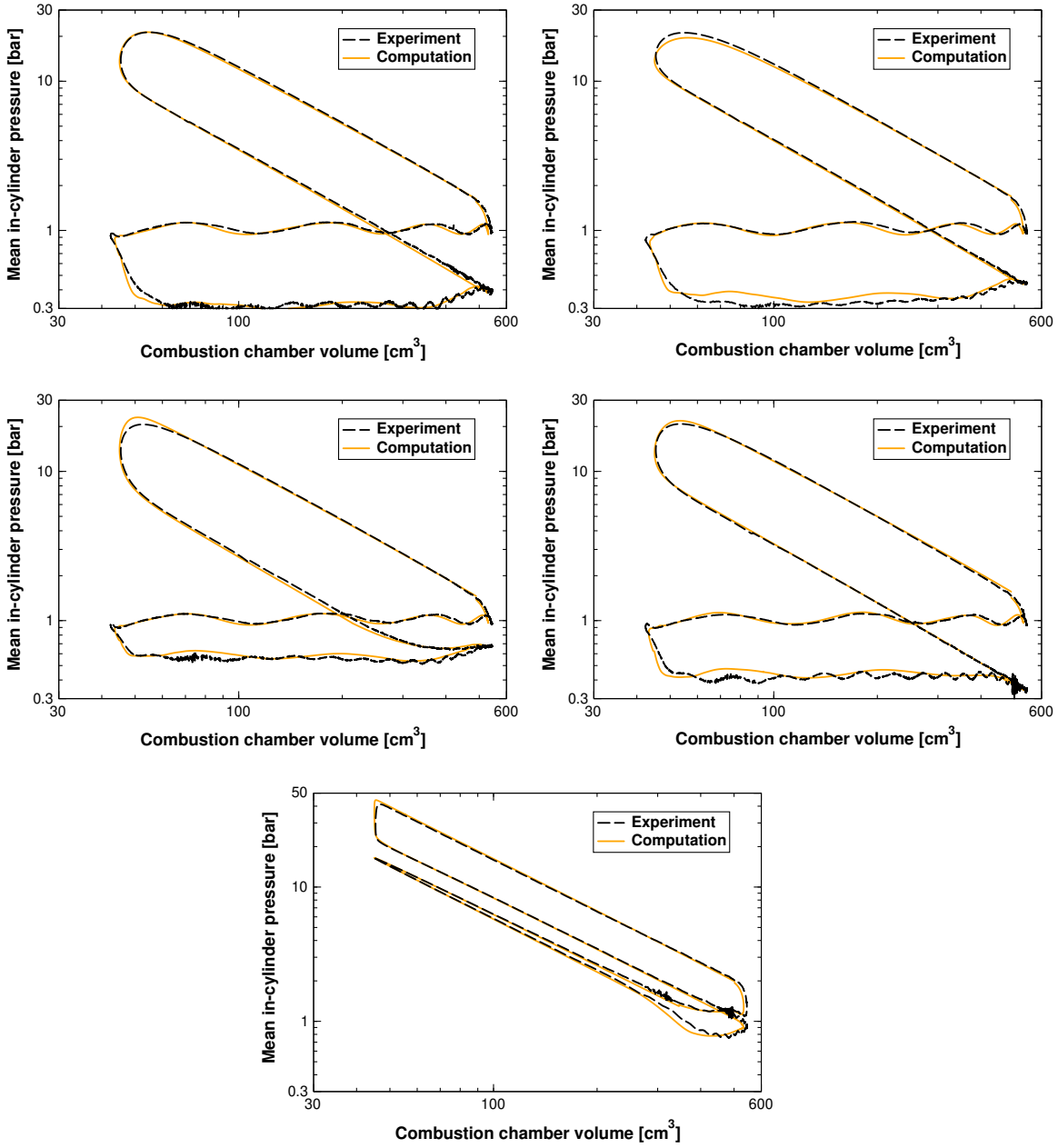

Fig. 3. Comparison in logarithmic scale of experimental (dashed line) and numerical (solid line) pressure–volume diagrams for all 5 operating strategies. Upper left: Reference SI operation. Upper right: Mixture leaning. Middle left: Atkinson cycle. Middle right: Miller cycle. Lower part: Controlled Auto-Ignition.

times. With a number of processors (8-core Intel Sandy Bridge E5-2670) ranging from 4 to 8 during the computation, results were obtained within 3 days on a per engine cycle basis.

5.2. Numerics validation

Before any in-depth analysis of engine behaviour with 3D CFD, a validation of the ability of the numerical tool to accurately reproduce experiments was necessary. For this purpose, the computation of complete engine cycles, starting with the exhaust stroke, allowed to check the convergence of numerical predictions towards experimental results. Experimental pressure measurements at the intake and exhaust sides defined boundary conditions and a carefully check of mass balances with air and fuel mass flow rate measurements validated the gas exchange modelling. The very good agreement with experiment (less than 1% difference on mass flow rates for all operating points) ensured trustworthy temperature predictions as long as pressure trace predictions were correct. Fig. 3 details such pressure trace predictions and compares the experimental and numerical $p-V$ diagrams for all 5 operating strategies. Numerics captured the alteration of pressure dynamics with changes of valve lift strategy, not only in the low pressure part of the cycle (gas exchange part), but also in the high pressure part of the cycle (compression stroke and combustion process). The latter ensured accurate initial conditions for combustion description and a sound basis for the analysis of the influence of thermodynamic conditions on combustion progress. Dedicated in-house models described combustion progress, be it for flame propagation [27,28] or for auto-ignition-induced kinetically-controlled heat release [29], and comparison with experiment confirmed their

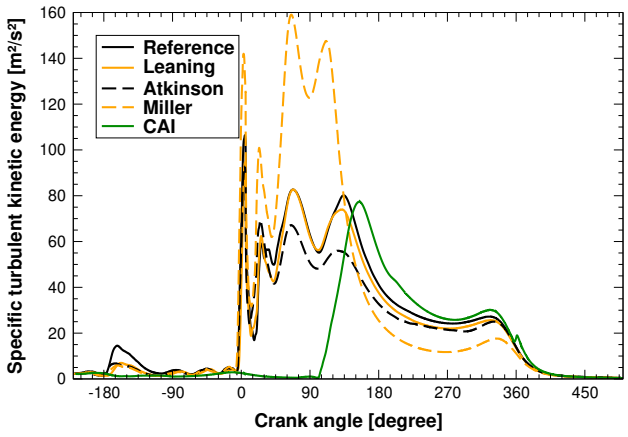

Fig. 4. Operating strategy influence on specific turbulent kinetic energy.

validity. This validation process ensured that present 3D CFD results were trustworthy data for a detailed analysis of involved phenomena.

6. Engine behaviour details

We analysed detailed engine behaviour based on 3D CFD results and summarised the main conclusions in the present section. Therefore, unless otherwise stated, results presented herebelow were extracted from 3D CFD results, while previously-detailed results were experimental measurements.

6.1. Strategy influence on in-cylinder turbulence

Fig. 4 details the influence of operating strategy on specific turbulent kinetic energy. Turbulence level analysis relied on specific turbulent energy *tke* instead of absolute turbulent kinetic energy *TKE* because it is more representative of flame/turbulence interaction that is mainly dependent on turbulent velocity u' ($tke = \frac{2}{3}u'^2$). Concretely, mixture leaning increased absolute turbulent kinetic energy because of the larger aspirated air mass but did not significantly modify specific turbulent kinetic energy as flow structure was not really different.

Valve strategy alteration for SI operation always lead to a loss in specific turbulent kinetic energy at spark timing. LIVC (Atkinson cycle) induced a slight reduction in specific turbulent kinetic energy during the whole intake stroke and some structured flow motion destruction during the backflow period. However, the turbulence loss at spark timing was limited. On the other hand, EIVC, obtained with a lower peak intake valve lift, created a far larger turbulence intensity during the intake stroke (larger flow velocities through intake valve curtain) but suffered from a more intense turbulence dissipation as soon as intake valves closed. Consequently, specific turbulent kinetic energy at spark timing was significantly lower than for any other operating point.

The most favourable strategy to turbulence intensity near Top Dead Centre (TDC) was the negative valve overlap strategy used to promote CAI combustion mode. Air aspiration was late in the intake stroke but with large velocities as peak intake valve lift was small. Consequently, we obtained the same benefit in turbulence generation as for Miller cycle but without any deficit in turbulence dissipation related to EIVC. However, this higher turbulence level had almost no direct influence on combustion speed since turbulence does not directly influence heat release for CAI combustion mode. Yet, the higher turbulence level had some indirect influence through heat losses to the walls that control mixture temperature stratification. A larger temperature distribution within the combustion chamber implies a longer delay between consecutive auto-ignitions at various places in the combustion chamber and therefore a longer combustion duration.

6.2. Strategy influence on late backflow

Changing the IVC timing and the intake pressure between operating strategies modified the late backflow intensity (or even occurrence). The expel of trapped burnt gases to the intake pipe at the end of intake stroke provided a way to quantify late backflow intensity, as no CO_2 flew in from the air path (Fig. 5).

Standard operation with intake valve closure 35 cad aBDC induced a slight backflow at the end of intake stroke (Fig. 5). The amount of burnt gases in the intake pipe remained low and only had a restricted influence on the following induction and combustion processes. Leaning the mixture did not alter flow motion, so that backflow remained similar to that of standard operation (Fig. 5).

With Miller cycle, intake valve closed early when the air was still inflowing, so that there was no backflow at all (Fig. 5). With Atkinson cycle, backflow was intended and large (Fig. 5). However, not only the intended air backflow occured but also a significant amount of burnt gases was expelled, so that burnt gas trapping from one cycle to the other included the recirculated gases through the intake circuit. This had to be correctly taken into account for accurate engine modelling, notably having a large enough volume in the modelled intake circuit so that burnt gases remained within the mesh and no hypothesis on composition at boundaries had to be done. We also had to perform some multicycle modelling as the extension of backflow could not be accurately predicted with any other tool than 3D CFD and could not therefore be specified as initial condition for the first cycle. For CAI operation, the short valve opening duration lead to the same behaviour as for Miller cycle: air was still inflowing at IVC (Fig. 5).

6.3. Strategy influence on mixture temperature

All operating strategies had distinctive mixture temperature histories (Fig. 6), which is a key point as temperature is the single most important quantity influencing the reactivity of the air–fuel mixture.

Mixture leaning lead to a significant increase in trapped mass during compression and expansion strokes (about 20% more air), which affected mixture temperature. Mixture temperature during compression stroke remained unchanged because neither the trapped gas temperature nor the effective compression ratio did change. On the contrary, the mass increase largely modified the temperature history during combustion and expansion stroke. The larger mass acted as a heat sink, so that end-of-combustion temperature and temperature during expansion were significantly lower, leading to lower NO_x emissions despite the favourable FAER value for NO_x production.

Both EIVC and LIVC implied a decrease in the effective compression ratio and therefore a lower temperature rise during compression stroke. However, the difference in intake valve closure timing with respect to BDC for best indicated efficiency lead to distinct temperature values at spark timing. Mixture temperature decrease at spark timing with respect to standard SI operation was very restricted for Miller cycle, only marginally affecting the laminar flame speed, despite the significant temperature reduction at BDC due to the expansion of trapped gases after IVC (see subfigure in Fig. 6). On the other hand, Atkinson cycle produced a reduction of around 100 K in mixture temperature at spark timing with respect to standard SI operation, which induced a massive laminar flame speed reduction of about 40%. The influence of EIVC or LIVC

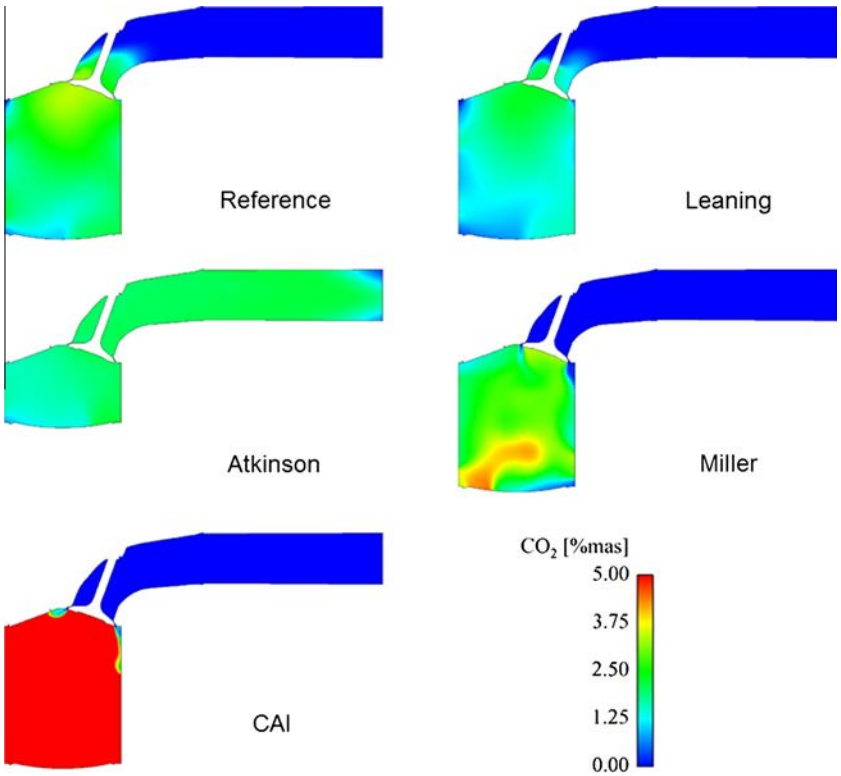

Fig. 5. Operating strategy influence on late intake backflow. CO_2 mass fraction is a tracer of backflow as there is no CO_2 in the inlet flow but CO_2 is present in the combustion chamber at intake valve opening.

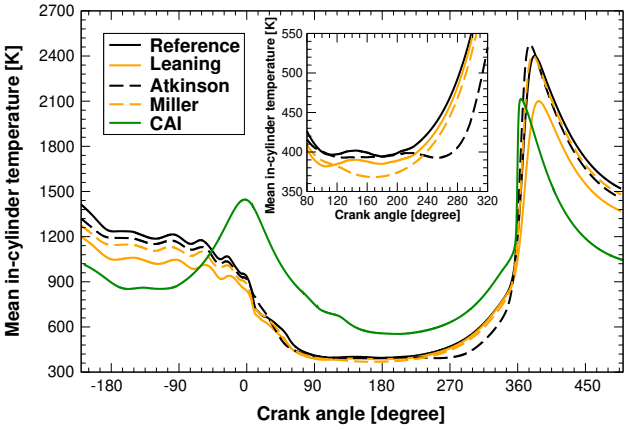

Fig. 6. Operating strategy influence on mean in-cylinder temperature.

on combustion speed was therefore totally different because of the distinct effects on the flame/turbulence interaction, as will be detailed in the following section.

CAI combustion mode also produced a very specific temperature history. The trapping of a large amount of burnt gases (55.8%mas of burnt gases in the mixture during compression stroke) to promote with heat the auto-ignition of the air–gasoline mixture did increase the mixture temperature during most of the engine cycle. Burnt gases were trapped with a truncated exhaust stroke, so that a burnt gas compression occured during the negative valve overlap producing high pressure and temperature values. The negative valve overlap duration was long (about 180 cad) because burnt gas compression required a late intake valve opening to avoid through expansion a massive burnt gas backflow into the intake pipe at intake valve opening. Nevertheless, despite expansion, trapped burnt gas temperature was high and ensured the survival of a significant heating during the intake and compression strokes. The large dilution effect of burnt gas trapping had the same heat sink effect as the enlarged trapped mass for mixture leaning: temperature during combustion and expansion stroke was significantly lower, drastically reducing NO_x formation.

6.4. Strategy influence on heat release

Fig. 7 compares heat release history for all operating points. On the one hand, switching from SI operation to CAI operation significantly increased mixture reactivity, to a point where combustion-induced noise level could become an issue. On the other hand, any change in operating strategy while maintaining SI operation produced an important loss in reactivity, restricting the indicated

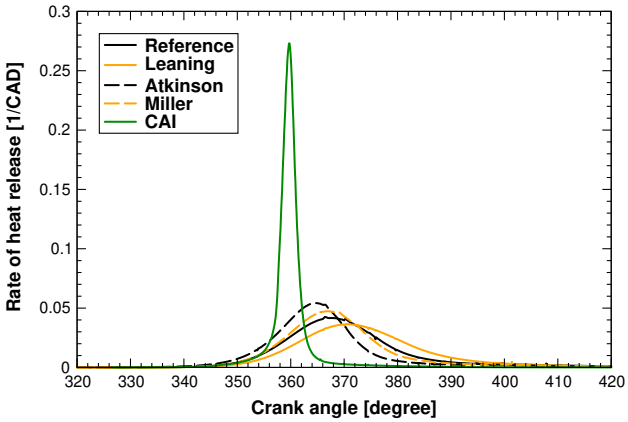

Fig. 7. Operating strategy influence on rate of heat release.

efficiency benefit. We experimentally adapted spark timing to minimum value for best torque, which hid reactivity trends and required numerical inputs to explain why further dethrottling was impossible because of combustion degradation.

The changes in reactivity for SI operation are mostly related to the interaction between flame and turbulence. The key parameter on the flame side is the laminar flame speed (S_L), that is mostly affected by the local fuel/air equivalence ratio and the mixture temperature as well as to a secondary level by in-cylinder pressure. As observed previously, changing the valve strategy also modified the specific turbulent kinetic energy, the key parameter explaining the flame speed enhancement by turbulence through flame wrinkling. With selected operating strategies, all 4 inputs (fuel/air equivalence ratio, temperature, pressure and turbulence) never changed simultaneously, and therefore never acted simultaneously on combustion speed.

To analyse the individual influence of each controlling parameter, we computed the evolution with operating conditions of the turbulent flame speed (S_T) at spark timing. Following Abdel-Gayed [34], S_T directly depends on the turbulent velocity u' (turbulence influence) and on the laminar flame speed S_L (chemistry influence) through Eq. (1):

$$\frac{S_T}{S_L} = 1 + \frac{u'}{S_L} \tag{1}$$

The computed specific turbulent kinetic energy provided the turbulence influence while laminar flame speed computations at given pressure, temperature and fuel/air equivalence ratio values indicated the chemistry influence. A proper selection of conditions for laminar flame speed computations performed with Chemkin solver provided the individual influence of each quantity as well as their combined effect. The quantification of the influence of each individual quantity helped identify the controlling parameters for each operating strategy.

To compare mixture leaning S_T to standard operation S_T, we computed all operating points from the FAER sweeping used to define the optimum leaning and extracted *tke* values, FAER values, mixture pressures and temperatures at spark timing. Results showed that specific turbulent kinetic energy and mixture temperature remained similar for all FAER values, so that only fuel/air equivalence ratio and, to a lower extent, pressure dictated S_T evolution. Fig. 8 details the individual negative influence of mixture leaning and pressure on turbulent combustion speed, keeping all

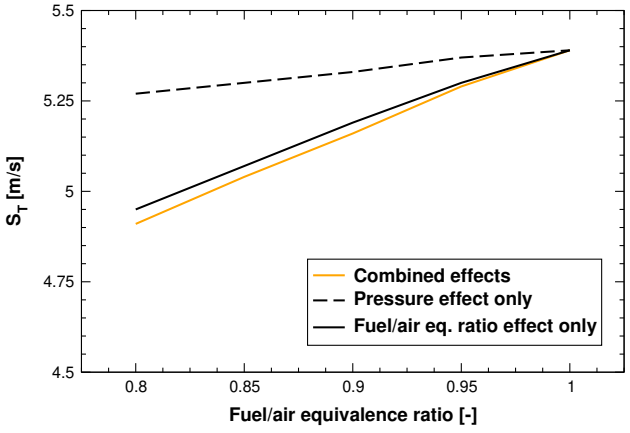

Fig. 8. Evolution of turbulent flame speed with mixture leaning. Black curves detail the individual influence of the main controlling parameters: fuel/air equivalence ratio (solid line) and pressure (dashed line); orange curve provides the combined effects of all controlling parameters. (For interpretation of the references to colour in this figure legend, the reader is referred to the web version of this article.)

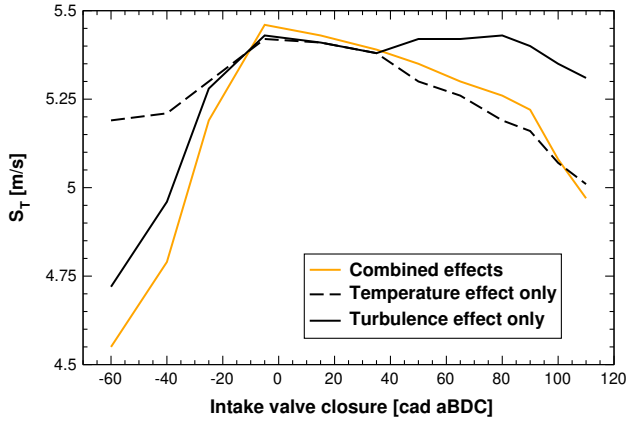

Fig. 9. Evolution of turbulent flame speed with intake valve closure timing. Black curves detail the individual influence of the main controlling parameters: turbulence (solid line) and temperature (dashed line); orange curve provides the combined effects of all controlling parameters. (For interpretation of the references to colour in this figure legend, the reader is referred to the web version of this article.)

other quantities identical to the stoichiometric conditions. A leaner mixture produces a lower laminar flame speed, which produces a slower heat release for a similar turbulence level. A higher pressure also slows down the laminar flame speed but the effect remains significantly more restricted than the effect of fuel depletion (Fig. 8). Both effects cumulated as mixture leaning increased pressure at spark timing. The selected fuel/air equivalence ratio for analysis (FAER of 0.8) is the leaner mixture beyond which combustion degradation became large enough to compensate for any further benefit in pumping losses and mixture thermodynamic properties, so that fuel economy degraded anew.

Similarly, to study the influence of the variation in intake valve closure timing, we computed all operating points from the IVC sweepings used to identify the best EIVC and LIVC timings and extracted *tke* values, FAER values, mixture pressures and temperatures at spark timing. Results showed that for such operating strategies, both mixture temperature and turbulence varied and did so in distinct proportions. For EIVC, turbulence dropped while temperature only slightly decreased. The lower reactivity was therefore a consequence of less flame propagation enhancing by turbulence. For LIVC, the loss in turbulence intensity was modest but mixture temperature dropped. The lower reactivity was therefore mainly a consequence of a lower laminar flame speed. To confirm this analysis and to provide a quantitative information, Fig. 9 depicts the evolution of the turbulent flame speed S_T at spark timing as a function of the intake valve closure timing. The cumulative effect of temperature and turbulence was difficult to analyse as the curve was not monotonic, explaining the addition of curves providing the individual influence of temperature and turbulence intensity. In both cases, the non-varying input (temperature or turbulent velocity) was set equal to the value at a standard intake valve closure (35 cad aBDC in the present study). Fig. 9 clearly indicates that on the LIVC side the predominant effect was temperature drop, explaining more than 90% of the evolution. On the other hand, the trend was less obvious on the EIVC side. For an intake valve closure just before BDC, temperature was the predominant parameter and the S_T value decreased as the S_L value dropped with temperature. However, for an earlier closure, both temperature and turbulence dropped, with turbulence becoming the predominant factor.

For Atkinson cycle (LIVC), combustion becomes slower because the mixture is cooler, which could be compensated for by intake air heating or turbulence increase with intake port redesign. For Miller

cycle (EIVC), however, turbulence is naturally dissipated whatever the port design, so that even if mixture temperature increases, a deficit in combustion speed remains.

This laminar and turbulent flame speed quantification indicates that turbulent flame propagation restricts operation strategy adaptation. For operating conditions that did not affect specific turbulent kinetic energy, there was no difference between reducing laminar flame speed through mixture temperature (Atkinson cycle) or through fuel/air equivalence ratio (mixture leaning): combustion degradation was too important when laminar flame speed was reduced by more than 0.4 m/s or by more than 30%. For Miller cycle, a large reduction in specific turbulent kinetic energy impeded the possible laminar flame speed reduction. Only a 0.1 m/s (7.5%) reduction in laminar flame speed was possible because the cumulative effects of laminar flame speed reduction and of turbulent velocity reduction lead to a 0.7 m/s reduction in turbulent flame speed. The larger reduction in turbulent flame speed resulted from the larger thermodynamic benefit on the remaining part of the cycle. Alternatively, considering a similar criterion on combustion stability for all strategies implied the same allowed total turbulent flame speed reduction of 0.4 m/s, be it through turbulence or through laminar flame speed.

6.5. Strategy influence on heat transfer

Wall temperature, mixture temperature and turbulence intensity mainly govern heat losses to the walls. We numerically estimated wall temperatures with a system simulation approach that was previously validated with wall temperature measurements on a similar engine setup. These computations indicated similar wall temperatures for all SI operating conditions, with only a slight reduction for lean operation. On the other hand, wall temperature increased for CAI operation but not in very large proportions as gas temperature was lower than for SI operation for expansion and exhaust strokes.

Based on mixture temperature and turbulence intensity differences, a large difference in heat transfer between SI operating points and CAI operating point was expected. Fig. 10 depicts the crank-based evolution of heat transfer during the complete cycle and confirms this expectation. The significantly higher mixture temperature combined with a larger turbulence intensity during compression stroke to produce higher heat losses for the CAI operating point. The lower mixture temperature during and after combustion reduced heat losses during expansion stroke but to too small an extent to compensate for the gap created during negative overlap as well as intake and compression strokes.

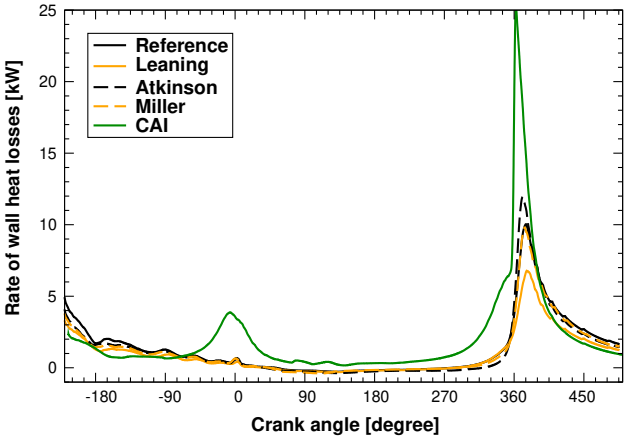

Fig. 10. Operating strategy influence on rate of heat losses to the walls.

Among SI operating points, there were some differences in heat transfer dynamics during the cycle but the global balance was very similar for all stoichiometric operating points. For lean operation, however, the benefit during combustion as well as during expansion and exhaust strokes was large enough to produce a global reduction of 20% in heat losses to the walls. It is noteworthy that despite some reduction in mixture temperature during compression stroke, EIVC and LIVC did not produce a sufficiently distinct temperature history to significantly reduce the overall heat losses, so that temperature reduction during compression was only a deficit for combustion speed and stability at part load without any benefit in heat losses.

6.6. Strategy influence on energy balance

Previous analyses indicated some pumping loss benefits for alternative valve strategies, some heat loss benefits for lean operation and some combustion-related cycle efficiency benefits for CAI operation. Furthermore, each strategy produced a different level of exhaust temperature, *i.e.* a different level of enthalpy losses to the exhaust. As there was no unique trend for each operating point, we performed a global energy balance to identify where were the benefits and drawbacks for each operating strategy. The results helped identify for which strategy any efficiency-oriented redesign was helpful or not.

Fig. 11 summarises the energy balance results for all 5 operating strategies. The display of the sources of energy consumption relies on fractions of the total fuel consumption of the reference operating point. As all operating points produced the same amount of torque, an identical 32% energy consumption ended into IMEP (indicated mechanical work). Fuel consumption benefit to obtain such an amount of torque appears as a lower cumulative sum of all sources of energy consumption. This type of display provides a fair comparison of both the relative and absolute variation of each source of losses. For example, in-cylinder heat losses to the walls were obviously far larger for CAI operation than for any SI operating point, be it on a relative or absolute basis.

Fig. 12 details the split of energy flows during the energy balance analysis. The first energy loss from gases in the combustion chamber is the pressure work on the piston (through the light green surface), indicated as mechanical work in Fig. 11. The second source of energy loss from gases in the combustion chamber are heat losses to the walls, namely to the piston (through the light green surface), the liner, the cylinder head and the valves (through

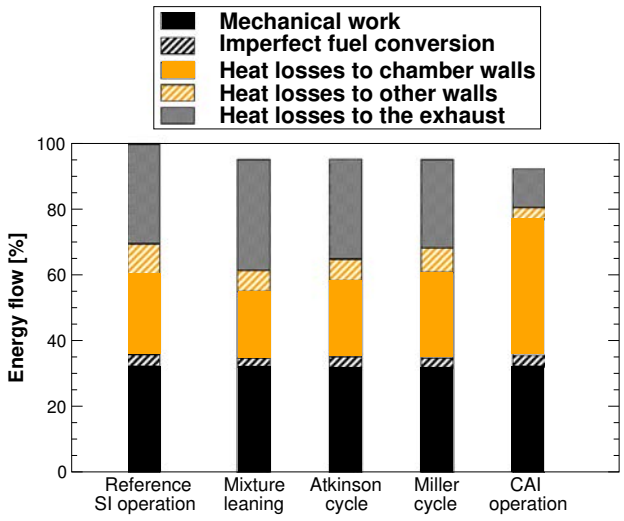

Fig. 11. Operating strategy influence on energy balance.

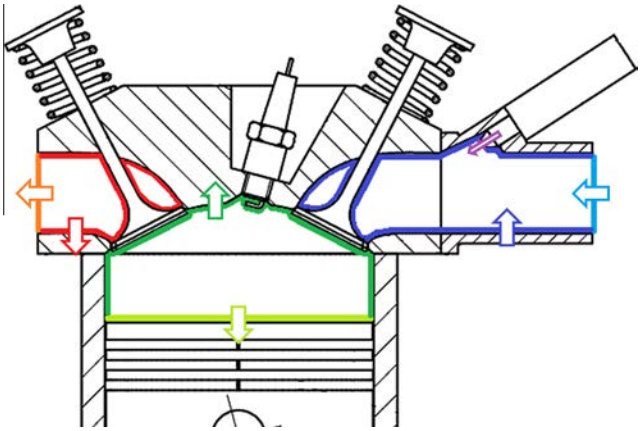

Fig. 12. Scheme of energy flow for energy balance analysis. Direction of arrows indicates the standard cycle-averaged direction for each energy flow.

the dark green surface). The energy balance was not restricted to the combustion chamber but included the cylinder head, so that the enthalpy balance does not consider flow at valves but at cylinder head inlet and outlet (where temperature and pressure transducers, as well as 3D CFD boundaries were located). As a consequence, a second source of heat losses to the walls in the intake (dark blue and purple surfaces) and exhaust (red surface) pipes adds to the heat losses to the combustion chamber walls. Except for Atkinson cycle with a large backflow into the intake pipe, heat losses to the walls in the intake system were mostly a limited heating of intake air by the walls. The contribution of intake pipe into this part of the energy balance was therefore secondary, except for LIVC. The energy balance between aspirated (through light blue and purple surfaces) and expelled (through orange surface) gases was further split into two parts. The first part was the contribution of partial combustion, leading to unburnt hydrocarbon and carbon monoxide emissions, which was a second order contribution. The main contribution was the heat losses to the exhaust in the form of hot expelled gases produced based on the cool aspirated air and fuel.

Fig. 11 indicates that all alternative SI operating strategies provided efficiency benefits with respect to standard operation (smaller cumulative sum) but mostly without massively changing the shape of the energy balance diagram. On the other hand, shifting from SI operation to CAI operation completely modified the weights of energy consumption sources, indicating a need for a complete rethinking of engine design updates for further gains.

For standard SI operation, a third of injected energy was converted into indicated mechanical work, a third flowed out of the engine as hot burnt gases and a third heated up the cooling fluids. Leaning the mixture reduced mixture temperature during combustion, expansion stroke and exhaust stroke, so that less heat was wasted into the cooling fluids. However, despite the lower temperature of the hot expelled gases (lower specific enthalpy), the gain in specific enthalpy was lower than the increase in exhaust mass flow rate, so that the absolute energy flow to the exhaust increased, reducing the expected benefits. Atkinson cycle did not bring any benefit in energy loss to the exhaust (neither by pollutant emissions, nor by heat flow) but induced some slight benefits in heat losses to the walls in the combustion chamber (−7%) as well as large benefits in heat losses to the walls outside the combustion chamber (−50%). Note that this latter effect was partly related the backflow phenomenon to the intake during early compression stroke. On the contrary, the influence of Miller cycle on heat losses to the walls was weak but we obtained a 12% benefit in enthalpy flow to the exhaust.

CAI operation produced a totally different energy balance. Dilution effect on mixture temperature during combustion as well as expansion and exhaust strokes and recirculation of hot burnt gases from one cycle to the other should provide large benefits in fuel consumption. Their combination lead to a significant reduction in energy loss to the exhaust as heat flow (−60% with respect to standard SI operation). Similarly, the low exhaust gas temperature lead to lower heat losses to the walls in the exhaust system (−60% with respect to standard SI operation). However, trapping large amounts of burnt gases into the combustion chamber significantly raised mixture temperature as intended but also significantly increased heat losses to the walls within the combustion chamber. The resulting increase of 70% in in-cylinder heat losses to the walls ate away at most of the ISFC benefits obtained on other phenomena, so that the final ISFC benefit was only 8%.

7. Conclusion

The analysis of various VVA strategies on a single part-load operating point indicated their drawbacks and explained why such approaches only brought restricted benefits with respect to the initial expectations. Changing valve strategy while maintaining SI operation degraded combustion because end-of-compression temperature drop decreased mixture reactivity and because turbulence dissipation restricted its beneficial effect on combustion speed. As mixture leaning also degraded combustion, no real synergy exists with VVA methods. Using VVA as a promoter for alternative combustion modes was a way to reach larger fuel consumption benefits but increased heat losses ate away at a large part of pumping loss and combustion efficiency benefits.

VVA was therefore a very efficient tool for pumping loss reduction but its actual implementation produced lower than expected benefits because of the increase in other cycle irreversibilities. Optimisation of fuel economy during SI operation appeared to be mainly combustion-limited, while CAI operation efficiency was mainly restricted by heat losses to the chamber walls. Improving efficiency for SI and CAI operation consequently requires very different counter-measures: increasing combustion speed on the SI side, reducing heat losses on the CAI side.

Acknowledgement

Authors would like to thank Florence Duffour for performing the strategy optimisation and for providing most of the experimental data.

References

[1] Luttermann C, Schünemann E, Klauer N. Enhanced valvetronic technology for meeting SULEV emission requirements. SAE Paper 2006-01-0849.
[2] Brüstle C, Schwarzenthal D. VarioCam plus – a highlight of the Porsche 911 Turbo engine. SAE Paper 2001-01-0245.
[3] Kojima S. Development of high-performance and low-emission gasoline engine. SAE Paper 2008-01-0608.
[4] Fujita T, Onogawa K, Kiga S, Mae Y, Akasaka Y, Tomogane K. Development of innovative Variable Valve Event and Lift (VVEL) system. SAE Paper 2008-01-1349.
[5] Bernard L, Ferrari A, Micelli D, Perotto A, Rinolfi R, Vattaneo F. Electrohydraulic valve control with MultiAir technology. Motortech Z 2009;70:4–10.
[6] Heinrich C, Scharrer O, Gebhard P, Pulcher H. Investigation of a 2-step valve train and its influence on combustion by means of coupled CFD simulation. SAE Paper 2005-01-0690.
[7] Scheidt M, Brands C, Kratzsch M, Günther M. Combined Miller/Atkinson strategy for future downsizing concepts. Motortech Z 2014;75:4–10.
[8] Kutlar OA, Arslan H, Calik AT. Methods to improve efficiency of four stroke, spark ignition engines at part load. Energy Convers Manage 2005;46:3202–20.
[9] Liu D, Wang T, Jia M, Wang G. Cycle-to-cycle variation analysis of in-cylinder flow in a gasoline engine with variable valve lift. Exp Fluids 2012;53:585–602.
[10] Millo F, Luisi S, Borean F, Stroppiana A. Numerical and experimental investigation on combustion characteristics of a spark ignition engine with an early intake valve closing load control. Fuel 2013;121:298–310.

[11] Grasreiner S. Combustion modeling for virtual SI engine calibration with the help of 0D/3D methods. Freiberg University. PhD thesis.
[12] Sellnau N, Kunz T, Sinnamon J, Burkhard J. 2-step variable valve actuation: system optimization and integration on a si engine. SAE Paper 2006-01-0040.
[13] Anderson MK, Assanis DN, Filipi ZS. First and second law analyses of a naturally-aspirated, Miller cycle, SI engine with Late Intake Valve Closure. SAE Paper 980889.
[14] Wan Y, Du A. Reducing part load pumping loss and improving thermal efficiency through high compression ratio over-expanded cycle. SAE Paper 2013-01-1744.
[15] Li T, Gao Y, Wang J, Chen Z. The Miller cycle effects on improvement of fuel economy in a highly boosted, high compression ratio, direct-injection gasoline engine: EIVC vs. LIVC. Energy Convers Manage 2014;79:59–65.
[16] Miklanek L, Vitek O, Gotfryd O, Klir V. Study of unconventional cycles (Atkinson and Miller) with mixture heating as a means for the fuel economy improvement of a throttled SI engine at part load. SAE Paper 2012-01-1678.
[17] Atashkari K, Nariman-Zadeh N, Gölcü M, Khalkhali A, Jamali A. Modelling and multi-objective optimization of a variable valve-timing spark-ignition engine using polynomial neural networks and evolutionary algorithms. Energy Convers Manage 2007;48:1029–41.
[18] Mahrous AFM, Potrzebowski A, Wyszynski ML, Xu HM, Tsolakis A, Luszcz P. A modelling study into the effects of variable valve timing on the gas exchange process and performance of a 4-valve DI homogeneous charge compression ignition (HCCI) engine. Energy Convers Manage 2009;50:393–8.
[19] Allen J, Law D. Production electro-hydraulic variable valve-train for a new generation of I.C. engines. SAE Paper 2002-01-1109.
[20] Duffour F, Vangraefschèpe F, Knop V, de Francqueville L. Influence of the valve-lift strategy in a CAI engine using exhaust gas re-breathing. Part 1: Experimental results and 0D analysis. SAE Paper 2009-01-0299.
[21] Knop V, de Francqueville L, Duffour F, Vangraefschèpe F. Influence of the valve-lift strategy in a CAI engine using exhaust gas re-breathing. Part 2: Optical diagnostics and 3D CFD results. SAE Paper 2009-01-0495.
[22] Duffour F, Knop V, Vangraefschèpe F, Leone T, Pascal V. Quantifying benefits of dual cam phasers, lean mixture and EGR on the operating range and fuel economy of a PFI NVO CAI engine. SAE Paper 2010-01-0844.
[23] Osborne RJ, Li G, Sapsford SM, Stokes J, Lake TH, Heikal MR. Evaluation of HCCI for future gasoline powertrains. SAE Paper 2003-01-0750.
[24] Woschni G. Universally applicable equation for the instantaneous heat transfer coefficient in the internal combustion engine. SAE Paper 670931.
[25] Bohbot J, Gillet N, Benkenida A. IFP-C3D: an unstructured parallel solver for reactive compressible gas flow with spray. Oil Gas Sci Technol 2009;64:309–35.
[26] Colin O, Truffin K. A spark ignition model for large eddy simulation based on an FSD transport equation (ISSIM-LES). Proc Combust Inst 2011;33:3097–104.
[27] Duclos J-M, Zolver M, Baritaud T. 3D modeling of combustion for di-si engines. Oil Gas Sci Technol 1999;54:259–64.
[28] Hélie J, Trouvé A. A modified coherent flame model to describe turbulent flame propagation in mixtures with variable composition. Proc Combust Inst 2000;28:193–201.
[29] Knop V, Michel J-B, Colin O. On the use of a tabulation approach to model auto-ignition during flame propagation in SI engines. Appl Energy 2011;88:4968–79.
[30] Knop V, Nicolle A, Colin O. Modelling and speciation of nitrogen oxides in engines. Proc Combust Inst 2013;34:667–75.
[31] Han Z, Reitz RD. Turbulence modeling of internal combustion engines using RNG k–ϵ models. Combust Sci Technol 1995;106:267–95.
[32] Kays WM, Crawford ME. Convective heat and mass transfer. 3rd ed. McGraw-Hill; 1994.
[33] Velghe A, Gillet N, Bohbot J. A high efficiency parallel unstructured solver dedicated to internal combustion engine simulation. Comput Fluids 2011;45:116–21.
[34] Abdel-Gayed RG, Bradley D, Lawes M. Turbulent burning velocities: a general correlation in terms of straining rates. Proc S Roy Lond A 1987;414:389–413.